

#### **OPEN ACCESS**

EDITED BY
Hamid Mirzaei,
University of Texas MD Anderson Cancer
Center. United States

REVIEWED BY
Zongde Zhang,
Southwest Medical University, China
Zhaohua Hou,
Memorial Sloan Kettering Cancer Center,
United States

\*CORRESPONDENCE
Dannel Yeo
Adannel.yeo@sydney.edu.au

RECEIVED 22 June 2025 ACCEPTED 24 September 2025 PUBLISHED 08 October 2025

#### CITATION

Liang O, White AL, Fielder T, Shin J-S, Sagnella SM, Schmitz U and Yeo D (2025) High mesothelin expression is associated with low cytotoxic T cell infiltration in pancreatic cancer.

Front. Immunol. 16:1651687.
doi: 10.3389/fimmu.2025.1651687

### COPYRIGHT

© 2025 Liang, White, Fielder, Shin, Sagnella, Schmitz and Yeo. This is an open-access article distributed under the terms of the Creative Commons Attribution License (CC BY). The use, distribution or reproduction in other forums is permitted, provided the original author(s) and the copyright owner(s) are credited and that the original publication in this journal is cited, in accordance with accepted academic practice. No use, distribution or reproduction is permitted which does not comply with these terms.

# High mesothelin expression is associated with low cytotoxic T cell infiltration in pancreatic cancer

Oliver Liang<sup>1,2</sup>, Amy L. White<sup>1,2</sup>, Timothy Fielder<sup>3</sup>, Joo-Shik Shin<sup>3,4</sup>, Sharon M. Sagnella<sup>1,5</sup>, Ulf Schmitz<sup>4,6</sup> and Dannel Yeo<sup>1,2,5\*</sup>

<sup>1</sup>Precision Oncology Laboratory, Cancer Innovations, Centenary Institute, Sydney, NSW, Australia, <sup>2</sup>School of Medical Sciences, Faculty of Medicine and Health, The University of Sydney, Sydney, NSW, Australia, <sup>3</sup>Department of Tissue Pathology and Diagnostic Oncology, Royal Prince Alfred Hospital, NSW Health Pathology, Sydney, NSW, Australia, <sup>4</sup>Central Clinical School, Faculty of Medicine and Health, The University of Sydney, Sydney, NSW, Australia, <sup>6</sup>Cell and Molecular Therapies, Royal Prince Alfred Hospital, Sydney Local Health District, Sydney, NSW, Australia, <sup>6</sup>Computational Biomedicine Lab, College of Science and Engineering, James Cook University, Townsville, OLD, Australia

**Objectives:** Mesothelin (MSLN) is a cell-surface glycoprotein overexpressed in the majority of pancreatic ductal adenocarcinoma (PDAC) cases and represents a promising immunotherapeutic target. Despite studies and clinical trials investigating MSLN-targeted immunotherapies, its biological role in PDAC carcinogenesis and influence on the tumor microenvironment remain poorly characterized. This study aims to investigate MSLN expression patterns in PDAC and assess their relationship to clinical outcomes and the immune microenvironment.

**Methods:** MSLN expression in 74 PDAC patients was evaluated by immunohistochemistry staining on a tissue microarray and correlated with clinicopathological features and survival outcomes. Complementary analyses of publicly available transcriptomic datasets (bulk RNA-seq and single-cell RNA-seq) were performed to characterize associations between MSLN expression and the tumor immune microenvironment with immunohistochemical validation.

**Results:** High MSLN expression (H-score  $\geq$  62) was associated with improved relapse-free survival (p = 0.021) and with increased patient age (p = 0.036). Transcriptomic analyses revealed high MSLN expression was associated with an immunosuppressive microenvironment characterized by reduced immune reactivity and diminished cytotoxic T cell infiltration. Immunohistochemical validation confirmed a trend toward decreased stromal cytotoxic T cell abundance with increasing MSLN expression.

**Conclusion:** This study revealed an inverse relationship between MSLN expression and cytotoxic T cell infiltration in PDAC, despite a trend toward improved relapse-free survival in MSLN-high tumors. These findings have important implications for MSLN-targeted immunotherapies and suggest that addressing the immunosuppressive microenvironment may be necessary to optimize their current responses in PDAC.

KEYWORDS

biomarker, microenvironment, immunosuppression, immunotherapy, precision medicine

### 1 Introduction

Pancreatic ductal adenocarcinoma (PDAC), accounting for more than 90% of all pancreatic malignancies, is an aggressive and lethal cancer (1). PDAC has a poor prognosis with a rising incidence rate and a high mortality rate (five-year survival of less than 10%) (2, 3). The majority of PDAC cases arise from microscopic dysplastic lesions known as pancreatic intraepithelial neoplasms (PanINs) (4), although other cystic precursor lesions, such as intraductal papillary mucinous neoplasms (IPMNs) and mucinous cystic neoplasms (MCNs), can also become malignant (5). Diagnosis occurs late in the majority of PDAC patients due to both the absence of specific clinical symptoms during early disease and the inherent challenges in imaging and detecting early-stage pancreatic tumors (6, 7). Although surgical resection is the only potentially curative treatment, most patients are diagnosed with locally advanced or metastatic disease and as such, are not eligible for resection. Standard systemic chemotherapy and radiotherapy have shown limited efficacy to date, highlighting the need for more effective therapies (8, 9).

MSLN is a glycosylphosphatidylinositol (GPI)-anchored glycoprotein that is overexpressed in certain solid tumors including PDAC, with minimal expression in normal tissues. Anti-MSLN immunotherapies, such as antibody-based therapeutics (10–12), immunotoxins (13), antibody-drug conjugates (14), and chimeric antigen receptor (CAR) T cells (15–17), have been evaluated in clinical trials. Despite promising preclinical results (18–20), clinical response to anti-MSLN immunotherapies remains modest (21, 22). Efforts are ongoing to better understand the underlying cause of treatment failures and to improve the effectiveness of the therapy.

The clinical significance of MSLN expression has been studied in PDAC as well as other cancer types including colorectal cancer (23, 24), ovarian cancer (25, 26), breast cancer (27, 28), gastric cancer (29, 30), lung cancer (31, 32), and mesothelioma (33, 34). However, there are conflicting results on the prognostic potential of MSLN due in part to differences in cohorts and methodologies used. Cohorts from the United States and Japan have reported an unfavorable association with tumor pathology and/or survival outcomes based on MSLN transcript (35, 36) and protein (37, 38) levels. Although no survival analysis was undertaken, no association was found between MSLN expression in PDAC tissues and clinicopathological factors (age, sex, disease stage, and tumor differentiation) in one cohort from China (39). No studies, to date, have performed immunohistochemical evaluation of MSLN in an Australian PDAC cohort.

In addition to its therapeutic and clinical significance, the biological importance of MSLN remains poorly understood. Under normal physiological conditions, MSLN is lowly expressed in mesothelial cells of the pleural, peritoneal, and pericardial lining (40). The

physiological function of MSLN remains elusive, as MSLN knockout mice do not display abnormalities in survival, development or reproduction (41). In cancer, MSLN is involved in various pathways that promote tumorigenesis. PDAC cells overexpressing MSLN promote proliferation by activation of STAT3 (42). MSLN signals through the PI3K/Akt pathway to increase autocrine IL-6 production and protect PDAC cells from TNF-alpha induced apoptosis (43–45). MSLN also binds to mucin-16 (MUC16) to facilitate the migration and metastatic dissemination of PDAC cells (46, 47).

Recent transcriptomic studies found MSLN was associated with anti-tumor immunity. Studies in ovarian cancer and colorectal cancer demonstrated an association between high *MSLN* expression and an immunosuppressive tumor microenvironment (TME) (48, 49). In PDAC, high *MSLN* expression was associated with an increased stromal *CD274* (PD-L1) expression in classical B and basal-like subtypes, which could play a role in immune evasion (50, 51). Another study found that PDAC tumors with high *MSLN* expression had decreased infiltration scores of immune cell subsets (CD4 T cells, CD8 T cells, B cells, and dendritic cells) (36). These findings warrant further characterization of the PDAC tumor landscape to understand the role that MSLN plays in immune regulation.

In this study, we evaluated novel associations between MSLN expression patterns, at both transcript and protein levels, with clinical outcomes and the composition of the immune microenvironment in PDAC patients.

### 2 Materials and methods

## 2.1 Immunohistochemical staining and scoring

Human PDAC tissue microarrays (TMAs), comprising 74 PDAC patients and 14 patients with precursor lesion (13 PanIN and 1 IPMN), were obtained through the Australian Pancreatic Cancer Genome Initiative (APGI) Bioresource (University of Sydney Human Research Ethics Committee: 2018/730). Serial human PDAC formalin-fixed paraffin-embedded (FFPE) sections were also obtained from 10 patients from the Royal Prince Alfred Hospital (RPA) (Sydney Local Health District Human Ethics Committee: 2020/ETH02321). MSLN IHC staining (clone MN-1, Rockland Immunochemicals, Pottstown, PA, USA) and analysis by H-score were undertaken, as previously described (34). Additionally on the serial FFPE sections, CD3 (clone LN10, Novocastra, Leica Microsystems, Deer Park, IL, USA), CD8 (clone C8144B, Dako, Santa Clara, CA, USA), and CD68 (clone KP1, Dako, Santa Clara, CA, USA) IHC staining were undertaken along with routine haematoxylin and eosin (H&E) staining. CD3, CD8, and CD68

scores were evaluated as percentage of stained cells within the tumor stromal area, as previously described (52). Two pathologists independently evaluated the staining, with final scores calculated as the average of their individual assessments.

### 2.2 Transcriptomic data preprocessing

Human PDAC bulk RNA-seq data was obtained from the European Genome-phenome Archive (EGA) database (International Cancer Genome Consortium (ICGC): DACO-7197). Two datasets containing 97 samples (ICGC PACA-AU; EGAD00001003298) and 219 samples (ICGC PACA-CA; EGAD00001003945) were included for analysis. To standardize read alignments across datasets, BAM files were converted to FASTQ using bedtools (ver.2.30.0) (53), and then realigned to the human genome assembly (GENCODE, release 35, GRCh38.p13) using STAR aligner (ver. 2.7.1a) (54). Raw gene counts were enumerated via featureCounts (ver.2.4.2) (55). Batch effects were corrected using the Combat\_seq function from sva (ver. 3.50.0) and only counts from protein-coding genes defined by the Human Genome Organisation Gene Nomenclature Committee (HGNC) were retained for analysis (56). Patients with missing clinical information were excluded as well as those with a diagnosis not classified as PDAC.

Mouse PDAC bulk RNA-seq data (n = 37 samples), from a published study (57), were obtained from the Gene Expression Omnibus (GEO) database (GSE109933). Raw read count data was filtered to remove non-protein-coding genes. Seven samples with unknown T cell infiltration status were excluded from the analysis.

Human PDAC single-cell RNA-seq (scRNA-seq) data were sourced from a published study (58). Data from 24 samples were collected as normalized gene expression matrices (Cancer Single-Cell Expression Map (CancerSCEM): https://ngdc.cncb.ac.cn/cancerscem/downloads), on the Genome Sequence Archive (CNCB-NGDC; PRJCA001063). Filtering was performed to retain only high-quality cells, as defined by cells with  $\geq 500$  detectable genes,  $\geq 1500$  unique molecular identifiers (UMI), > 0.8 cell complexity (log10 genes per UMI), and <10% of transcripts from mitochondrial genes.

### 2.3 Bulk RNA-seq data analysis

Normalization of raw gene counts and differential expression analysis were conducted via DESeq2 (ver. 1.38.2) (59). For the human dataset, samples in the top and bottom tertiles of MSLN expression were compared. Due to smaller sample size (n = 30), the mouse dataset was split based on median Msln expression and compared. Upregulated and downregulated genes were identified based on significance (adjusted P-value < 0.05) and expression changes (absolute log2 FC > 0.58). Over-representation analysis of upregulated and downregulated genes was conducted separately via Gene Ontology (GO) enrichment analysis in clusterProfiler (ver

4.7.1.003) (60). Results were visualized using the treeplot function via enrichplot (ver 1. 18.4).

Tumor reactivity was evaluated for human and mouse datasets using the tumor reactive gene signatures (TRS) derived from a previous study, which has been validated in melanoma and several other solid tumor datasets (61). For the mouse dataset, TRS genes were converted to mouse Ensembl IDs. TRS scores were calculated using GSVA (ver 1.46.0) with default parameters as previously described (62).

For estimates of cell type proportions, gene expressions from the human dataset were converted into Transcripts Per Million (TPM) values and analyzed using the "Immune Estimation" algorithm from TIMER2.0 (63).

### 2.4 scRNA-seq analysis

Integration, clustering, and dimensionality reduction of scRNAseq samples were performed via Seurat (ver 4.3.0) (64). Elbow plots were used to determine the optimal number of principal components (PCs), and PCs 1 to 30 were used for clustering at resolution = 0.5. Annotation was performed at single cell level via SCINA (ver 1.2.0) (65), using cell type identification markers in the original study from which the data was derived (58). Marker expression in each cell type was verified after cell annotation. Samples were assigned to high and low MSLN expression groups based on median cutoff of MSLN normalized counts per cell. For analysis of specific subtypes within annotated cell types, cell populations were isolated from the integrated dataset and reclustered at optimal resolution determined from a range of 0.5, 0.1, and 0.05. Manual annotation was performed for each cluster based on the expression of representative markers, which were identified using the FindAllMarkers function from Seurat (ver 4.3.0). UMAP (Uniform Manifold Approximation and Projection) plots were generated to illustrate cell clusters and specific marker expression across clusters using the DimPlot and FeaturePlot functions from Seurat (ver 4.3.0), respectively. A balloon plot of MSLN expression in annotated cell types across samples was generated using the ggballoonplot function in ggpubr (ver 0.6.0). For the macrophage population, M1 and M2 polarization scores were evaluated for each sample via UCell (ver 2.10.1), based on previously established M1 and M2 gene signatures (66, 67).

Differential gene expressions of CD8 T cell clusters from the MSLN-high and MSLN-low groups were assessed using the FindMarkers function based on default thresholds (adjusted P-value < 0.05 and absolute log2 FC > 0.25). Upregulated and downregulated genes were used in downstream GO enrichment analysis and visualized. Phenotypic profiling was performed using ProjecTILs (ver 3.5.1), with phenotypes inferred by projecting CD8 T cells onto the reference atlas of tumor-infiltrating CD8 T cells provided within the package (68). Cytokine signaling activities in CD8 T cells from each sample were evaluated using the CytoSig database via scaper (ver 0.2.0) (69). Expression levels of memory and exhaustion markers, as well as all chemokine and chemokine

receptors, were averaged for CD8 T cells from each sample and compared between the MSLN-high and MSLN-low groups.

### 2.5 Statistical analysis

Statistical analysis was performed in GraphPad Prism (ver 10.4.1, San Diego, California, USA) and R Statistical Software (ver 4.4.2, Vienna, Austria). Clinicopathological characteristics associations with MSLN expression from TMA data and RNA-seq data were evaluated using the Mann-Whitney U test for continuous variables, and the chisquared test for categorical variables. Survival data was analyzed using Kaplan-Meier curves with the log-rank test. Optimal H-score cutoff for survival using the exact distribution of maximally selected rank statistic was used, as previously described (70), using the surv cutpoint function from survminer (ver 0.5.0). Univariate and multivariate analyses were performed using Cox proportional hazards regression models for estimating hazard ratios (HR) with 95% confidence intervals (CIs). For multivariate analysis, effects of covariates (age, sex, and tumor stage) were accounted for when evaluating survival differences. Unpaired student's t-test and Pearson correlation analysis were used in other comparisons between two groups of continuous variables. In all cases, two-tailed tests were used, and statistical significance was set at p < 0.05.

### 3 Results

### 3.1 High MSLN is associated with increased relapse-free survival

The clinical characteristics of the 74 PDAC TMA patients are summarized in Table 1. Twelve of the patients (16.2%) received

TABLE 1 Demographic and clinicopathological summary of Australian PDAC patients in the tissue microarray cohort.

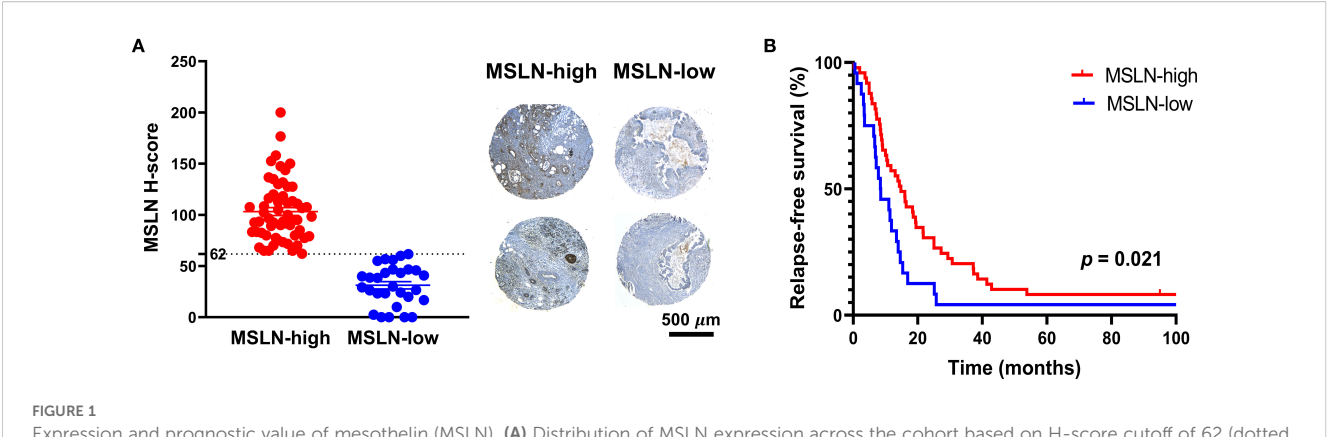
Parameter	Patient n (%)
Total	74 (100.0)
Age (years)	74 (100.0)
< 65	36 (48.6)
≥ 65	38 (51.4)
Sex	74 (100.0)
Male	39 (52.7)
Female	35 (47.3)
Tumor stage	72 (97.3)
IA	3 (4.2)
IB	8 (11.1)
IIA	20 (27.8)
IIB	38 (52.8)
IV	3 (4.2)

chemotherapy, as adjuvant (n = 7), neoadjuvant (n = 2), and/or palliative (n = 3) treatment. No difference in MSLN H-score was observed between the PDAC and the precursor lesion cohorts (14 patients consisting of PanINs and IPMNs) (Supplementary Figure S1A). Using an H-score cutoff of 62 (Supplementary Figure S1B), 32% (n = 24) were classified as MSLN-low and 68% (n = 50) were classified as MSLN-high (Figure 1A). The MSLN-high group had significantly higher relapse-free survival (RFS) with a median of 14.5 months (95% CI = 10.0 - 21.6 months), compared to a median RFS survival of 8.5 months (95% CI = 6.9 - 13.9 months) in the MSLN-low group (p = 0.021) (Figure 1B). The MSLN-high group had significantly reduced univariate HR (0.571, 95% CI = 0.343 - 0.951, p = 0.031) and reduced, albeit not significant, HR by multivariate analysis, adjusted for age, sex, and tumor stage (0.618, 95% CI = 0.332 - 1.147, p = 0.127). Clinicopathological associations with MSLN expression found that the MSLN-high group exhibited a positive association with increased age (p = 0.036) (Table 2). There was no difference between MSLN expression with respect to all other parameters examined including sex, tumor characteristics (stage, size, location, differentiation, and residual tumor), invasion (in peritoneum, and vasculature) and lymph node involvements.

Interestingly, no significant difference in patient outcomes (overall and relapse-free survival) was observed in relation to MSLN expression levels in the RNA-seq datasets (Supplementary Figure S2). The MSLN-high group did not correlate with any of the clinicopathological parameters examined, including age, sex, tumor characteristics (stage, location, and differentiation), treatment type, response, and relapse status (Supplementary Table S1). This discrepancy could be due to differences in MSLN expressions at transcript versus protein levels.

# 3.2 High MSLN is associated with reduced immune activity in human and mouse PDAC tumors

To investigate the biological significance of MSLN, transcriptomic analysis was conducted on human and mouse RNA-seq datasets to compare samples with high and low MSLN expressions (Figures 2A, B). In both datasets, the MSLN-high group exhibited downregulation of genes involved in immune-associated pathways, including the regulation of leukocyte adhesion, proliferation, and migration/ chemotaxis (Figures 2C, D). In addition, T cell activation and more broadly adaptive immune response pathways were downregulated. Within the top 30 downregulated pathways examined, the human RNA-seq dataset also included two clusters of pathways participating in bone development and peptide secretions, although these were not observed in the mouse RNA-seq dataset, which was comprised only of immune-associated clusters. To examine anti-tumor responses, tumor reactivity was predicted using tumor reactive CD8 T cell signature (TRS) scores from a previous study (61), which has been validated using hepatocellular carcinoma, non-small-cell lung cancer, melanoma, and colorectal cancer datasets. The MSLN-high group in both human and mouse datasets showed significantly lower TRS scores, indicating high MSLN expression is potentially associated with reduced antitumor immune responses (Figures 2E, F).

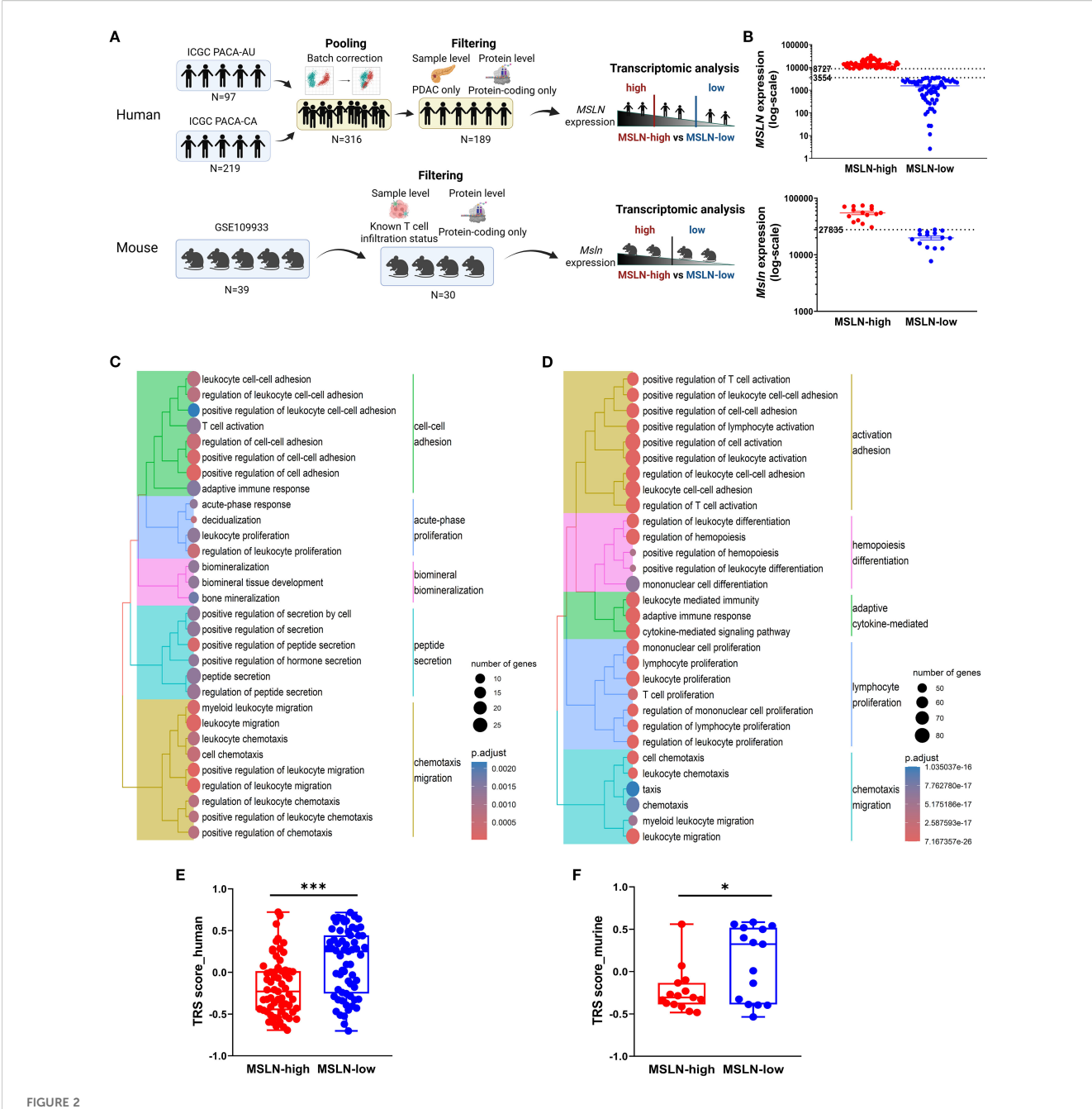


Expression and prognostic value of mesothelin (MSLN). (A) Distribution of MSLN expression across the cohort based on H-score cutoff of 62 (dotted line) (left). Mean  $\pm$  SEM. Representative images of tissue microarray samples from the MSLN-high and MSLN-low groups (right). Scale bar = 500  $\mu$ m. (B) Kaplan Meier curves of relapse-free survival of MSLN-high and MSLN-low groups. P-value was derived from log-rank test.

TABLE 2 Associations between mesothelin expression levels and clinicopathological characteristics of Australian PDAC patients in the tissue microarray cohort.

Parameter	Category	Total ( <i>n</i> = 74)	MSLN-high ( <i>n</i> = 50)	MSLN-low ( <i>n</i> = 24)	P-value
Age (years), median (range)		65 (40-83)	66.5 (44-79)	60.5 (40-83)	0.036
Sex, n (%) 74 (100.0)	Male	39 (52.7)	29 (58.0)	10 (41.7)	ns
	Female	35 (47.3)	21 (42.0)	14 (58.3)	
Tumor stage, n (%) 72 (97.3)	IA-IB	11 (15.3)	9 (18.4)	2 (8.7)	ns
	IIA	20 (27.8)	13 (26.5)	7 (30.4)	
	IIB - IV	41 (56.9)	27 (55.1)	14 (60.9)	
Tumor size, n (%) 64 (86.5)	≤ 3.5 cm	42 (65.6)	31 (68.9)	11 (57.9)	ns
	> 3.5 cm	22 (34.4)	14 (31.1)	8 (42.1)	
Tumor location, <i>n</i> (%) 55 (74.3)	Head	42 (76.4)	28 (73.7)	14 (82.4)	ns
	Body	4 (7.3)	3 (7.9)	1 (5.9)	
	Tail	9 (16.4)	7 (18.4)	2 (11.8)	
Tumor differentiation, n (%) 72 (97.3)	Well differentiated	8 (11.1)	6 (12.5)	2 (8.3)	ns
	Moderately differentiated	41 (56.9)	27 (56.3)	14 (58.3)	
	Poorly differentiated	23 (31.9)	15 (31.3)	8 (33.3)	
Residual tumor, <i>n</i> (%) 57 (77.0)	No residual tumor	32 (56.1)	18 (52.9)	14 (60.9)	ns
	Residual microscopic tumor	25 (43.9)	16 (47.1)	9 (39.1)	
Peritoneal invasion, <i>n</i> (%) 54 (73.0)	Absent	9 (16.7)	8 (20.0)	1 (7.1)	ns
	Present	45 (83.3)	32 (80.0)	13 (92.9)	
Vascular invasion, <i>n</i> (%) 35 (47.3)	Absent	14 (40.0)	11 (42.3)	3 (33.3)	ns
	Present	21 (60.0)	15 (57.7)	6 (66.7)	
Lymph nodes involved, <i>n</i> (%) 59 (79.7)	0	26 (44.1)	19 (47.5)	7 (36.8)	ns
	1-3	24 (40.7)	16 (40.0)	8 (42.1)	
	4-7	9 (15.3)	5 (12.5)	4 (21.1)	

MSLN, mesothelin; ns, not significant.



High mesothelin (human: *MSLN*, mouse: *Msln*) transcript is associated with decreased immune functions and tumor reactivity. (A) Workflow for transcriptomic analysis of human (top) and mouse (bottom) bulk RNA-sequencing datasets. (B) Human (top) and mouse (bottom) datasets were separated into MSLN-high and MSLN-low groups based on transcript expression of MSLN. Expression was quantified as normalized read counts (DESeq2). Expression thresholds for stratification are indicated (dashed lines). Top 30 biological processes from gene ontology enrichment analysis of downregulated genes in MSLN-high vs MSLN-low groups from the human (C) and mouse (D) datasets. Predicted tumor-reactive T cell signatures (TRS) scores for MSLN-high and MSLN-low groups from the human (E) and mouse (F) datasets. Statistical testing by student's t-tests (\*p < 0.05; \*\*\*p < 0.001; ns, not significant).

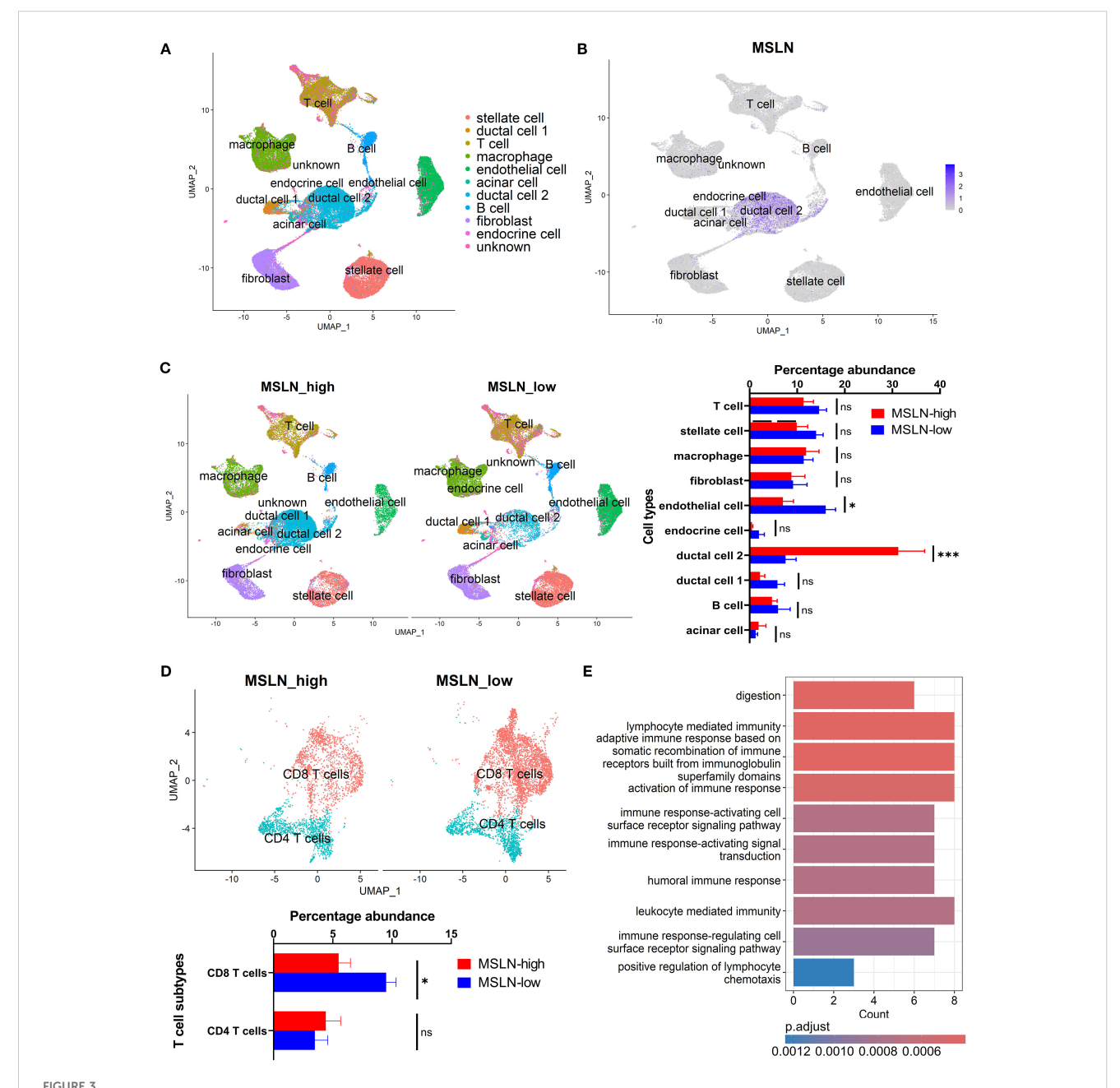
To investigate if immune cell infiltration into tumors also decreased, the relative proportions of key immune cell infiltrates (such as T cells and macrophages) were estimated via cell type prediction algorithms and compared between the MSLN-high and MSLN-low groups in the human RNA-seq dataset. However, strong discordance was observed across the algorithms (Supplementary Figure S3). For the mouse RNA-

seq dataset, T cell infiltration status of the implanted tumor clones, described in the study from which the mouse data was derived (57), was not associated with *Msln* expression. *Msln* expression did not differ significantly between "T cell high" and "T cell low" clones, nor did tumors in the MSLN-high group have higher proportions of "T cell high" clones (Supplementary Figure S4).

# 3.3 Cytotoxic T cells are reduced in PDAC tumors with high *MSLN* expression by single-cell RNA-seq

In the human scRNA-seq dataset, *MSLN* expression was mainly distributed in a malignant ductal 2 cell population, as demonstrated previously (58) (Figures 3A, B). Highest *MSLN* expression was also confirmed in the ductal 2 cells based on the intensity of expression

and percentage abundance (percentage out of total cells) in individual samples (Supplementary Figure S5). The MSLN-high group exhibited a significantly higher percentage of ductal 2 cells (mean  $\pm$  SEM:  $31.2\% \pm 5.5\%$  vs  $7.6\% \pm 2.2\%$ ) and lower percentage of endothelial cells (mean  $\pm$  SEM:  $7.0\% \pm 2.2\%$  vs  $16.0\% \pm 2.1\%$ ) (Figure 3C). Further characterization revealed a *MUC1*-positive cluster to be the predominant subtype of ductal 2 cells, but both the *MUC1*-positive and one of the *MUC1*-negative clusters showed



Characterization of human pancreatic cancer from single-cell transcriptomics based on mesothelin (MSLN) expression. (A) UMAP visualization showing the clustering of cells following integration of all samples. Cell type annotations represented by different colors. (B) Feature plot indicating the distribution of MSLN expression across the annotated cell clusters. Color scale shows the level of MSLN expression, with higher intensity indicating higher expression. (C) Comparison of the profiles of annotated cell types in MSLN-high and MSLN-low groups. Samples were stratified based on median MSLN normalized counts per cell. Overall landscape based on UMAP visualization (left) and quantified differences in percentage abundance (percentage out of total cells) of cell types (right). (D) T cell subtype profiles in the MSLN-high vs MSLN-low groups. (E) Bar plot of the top 10 downregulated biological processes from gene ontology analysis of CD8 T cells in MSLN-high vs MSLN-low groups. Mean  $\pm$  SEM. Statistical testing by student's t-tests (\*p < 0.05; \*\*\*p < 0.001; ns, not significant).

increased percentages abundance in the MSLN-high group (Supplementary Figure S6A). The endothelial cells were comprised of three clusters representing an arterial population and two (*PLVAP+/POSTN+*) venous populations (Supplementary Figure S6B). Reductions in percentage abundance were observed only in the *PLVAP+* venous subtype, which comprised the majority (~65%) of endothelial cells in MSLN-high vs MSLN-low groups.

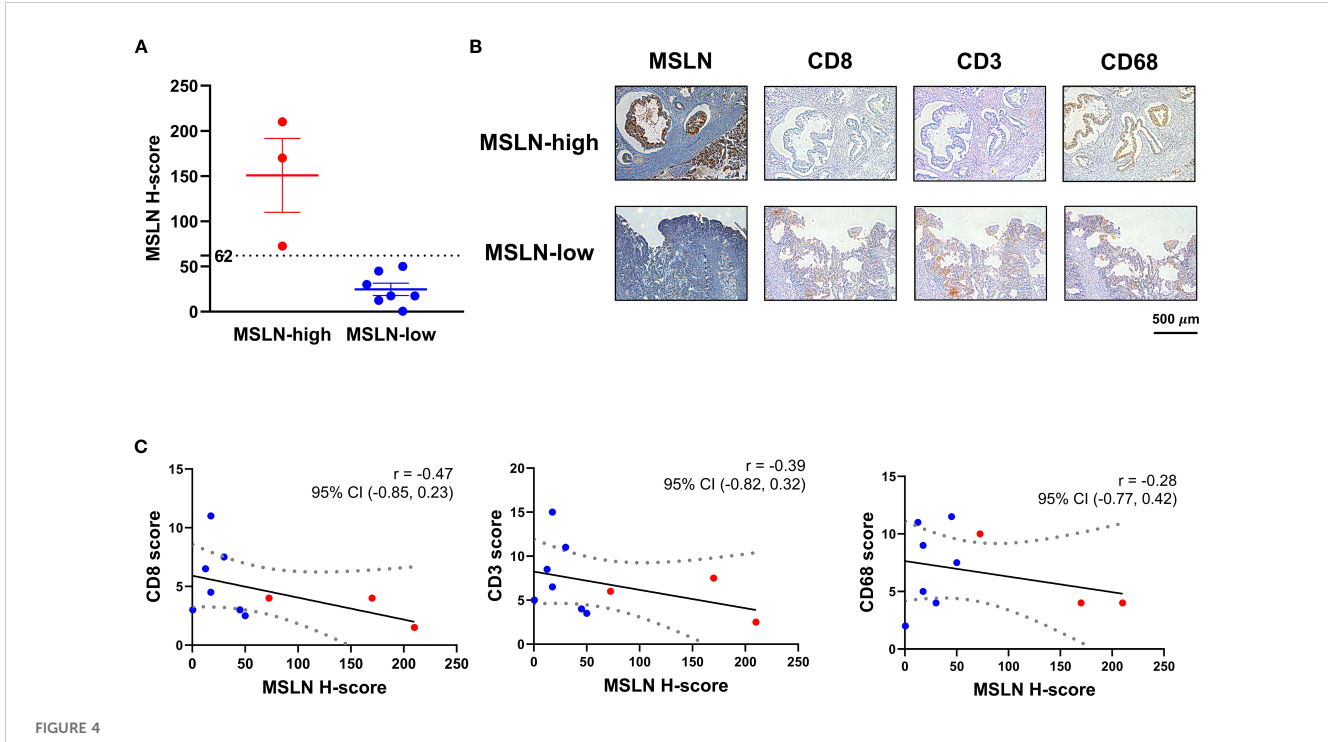
Although differences in global abundance of T cell infiltrates were not observed, the CD8 T cell subset showed significantly reduced percentage abundance in the MSLN-high group (mean  $\pm$  SEM: 5.5%  $\pm$  1.0% vs 9.5%  $\pm$  0.8%) (Figure 3D). This represents a more than 40% reduction in total CD8 T cell populations, when compared to the MSLN-low group. Other immune subsets (CD4 T cells, B cell and macrophage subsets) did not show any significant difference in percentage between MSLN-high and MSLN-low groups (Supplementary Figures S6C, D). However, within the macrophage population, the MSLN-high group demonstrated a shift towards an M2-polarized phenotype (Supplementary Figure S7).

Transcriptomic profiles of CD8 T cell subset in the MSLN-high group showed genes involved in immune-associated activity pathways to be downregulated compared to the MSLN-low group (Figure 3E). These pathways participate in adaptive immune responses, immune activation, and chemotaxis, consistent with the bulk RNA-seq analysis. The memory and exhaustion phenotypes, as well as cytokine and chemokine profiles, of CD8 T

cells were further characterized. No significant differences were observed in the memory or exhaustion phenotypes between MSLN-high and MSLN-low groups (Supplementary Figure S8). When compared to the MSLN-low group, CD8 T cells from MSLN-high group showed enrichment of GMCSF, HGF, IL-1, IL-2, and TNFSF12 signaling pathways (Supplementary Figure S9). These cells also showed downregulated expressions of chemokines *CCL2*, *XCL1*, and *XCL2*, as well as the chemokine receptor *CXCR6* (Supplementary Figure S10). However, expression of *CXCL5*, a neutrophil chemoattractant known to impair CD8 T cellmediated anti-tumor immunity (71), was upregulated. These findings suggest that high *MSLN* expression is associated with reduced abundance and altered transcriptomic activities of CD8 T cell infiltrates in PDAC.

## 3.4 Tumors with high MSLN expression show reduced cytotoxic T cell infiltration

To validate the transcriptomic relationship between MSLN expression and T cell infiltration, IHC staining on 10 surgically resected PDAC tumors was undertaken. MSLN expression (evaluated as H-score) showed a range from 0.5 – 210 (Figure 4A). Using the H-score cutoff of 62, the MSLN-high group (n=3) exhibited less intense, albeit not significant, staining of CD8 (mean  $\pm$  SEM:  $3.167 \pm 0.833$  vs  $5.429 \pm 1.172$ , p = 0.272) and



Associations of mesothelin (MSLN) expression with T cell infiltration in tumor stroma. (A) H-score distribution of MSLN staining on tissue sections from surgical specimens. Samples were stratified into MSLN-high and MSLN-low groups based on the H-score of 62. (B) Immunohistochemical (IHC) staining of representative serial FFPE sections from samples in the MSLN-high and MSLN-low groups. Scale bar = 500 µm. (C) Correlational analysis of MSLN H-score with CD8, CD3, and CD68 scores. Linear regression model was fitted (solid line), with dashed boundaries representing the 95% confidence interval (CI). Samples classified as MSLN-high (red) and MSLN-low (blue) groups were highlighted. Correlation coefficient (r) and its 95% CI were indicated for each pair-wise analysis.

CD3 (mean  $\pm$  SEM: 5.333  $\pm$  1.481 vs 7.643  $\pm$  1.580, p = 0.409) in the tumor stroma (Figure 4B; Supplementary Figure S11). CD68, used as a negative control, showed comparable staining between MSLN-high and MSLN-low groups (mean  $\pm$  SEM: 6.000  $\pm$  2.000 vs 7.143  $\pm$  1.366, p = 0.656). Across all samples, a decreasing trend was observed in all three (CD8, CD3, and CD68) scores with increasing MSLN H-score, but correlations did not reach significance (CD8: p = 0.174; CD3: p = 0.267; CD68: p = 0.432), likely due to low sample numbers (Figure 4C). Overall, a decreased trend in CD8 T cell infiltration was observed in MSLN-high tumors.

### 4 Discussion

This study identified high MSLN expression (H-score  $\geq$  62 from IHC staining) in PDAC to be associated with improved RFS and age. Transcriptomic analysis found a link between MSLN expression and an immunosuppressive tumor landscape. Specifically, CD8 T cells had reduced immune reactivity and reduced percentage abundance in PDAC tumors with high MSLN expression. In subsequent IHC validation, PDAC tumors with high MSLN expression demonstrated reduced infiltration of CD8 T cells in the stroma, although significance is not reached and confirmations in larger independent cohorts remain necessary.

The study identified MSLN as a biomarker for improved prognosis, which contrasts previous studies that found high MSLN expression to be correlated with worse survival outcome in PDAC (37, 38, 46). This discrepancy could be due to the different methodological classification and scoring used. Only one other study in PDAC used the H-score system for stratification. Using a median MSLN H-score cutoff of 180, they found poor survival in patients with high co-expression of MSLN and MUC16 (46). Other studies established cutoffs either based on the percentage of MSLNpositive cells alone (38) or the percentage of positive cells with the staining intensity analyzed separately (37). Antibody clones for MSLN staining also varied in studies. Two studies used anti-MSLN antibody clone 5B2 (37, 46), in contrast to the MN-1 clone used in the current study. The 5B2 clone has been found to have lower affinity and staining positivity in PDAC compared to the MN-1 clone (72). Staining patterns also differ between MN-1 and 5B2 clones, likely due to differential expression of epitopes for MSLN recognition, where the exact binding site for 5B2 has not been characterized (34).

Underlying cohort-specific factors can potentially contribute to the observed findings as well. Our TMA cohort is relatively small (n=74), with only a limited number of individuals receiving adjuvant chemotherapy (n=7) and having available resection margin data (n=56). Consequently, the effects of surgical resection and adjuvant chemotherapy on RFS could not be comprehensively examined in this cohort and were therefore excluded from the multivariate analysis, although they may represent potential confounders. Further investigation in a larger cohort and with biopsy samples are warranted.

Our study is the first to examine MSLN expression in an Australian PDAC population via IHC. Interestingly, high MSLN

expression, in tumors of an Australian mesothelioma patient cohort, was also associated with improved patient outcomes (34). In mesothelioma, the epithelioid subtype shows higher MSLN expression and a more favorable prognosis than the less differentiated sarcomatoid and biphasic subtypes (73). Although MSLN was not associated with the histological grade (Table 2), the relationship of MSLN expression with molecular subtypes of PDAC have not been examined in this Australian cohort, due to the lack of patient-matched transcriptomic data, and requires further investigation. Additionally, multiple proteases in the ADAM, MMP, and BACE families have been known to shed MSLN from cancer cells (74). Tumors with high MSLN expression could potentially be more resistant to antigen shedding, thus enabling greater surface antigen availability for immune surveillance, as MSLN-specific CD4 and CD8 T cells have been detected in the peripheral circulation of PDAC patients (75). Conversely, tumors with low cell-surface MSLN expression and high shedding activity may release elevated levels of soluble MSLN into the circulation, where sustained exposure could contribute to T cell anergy over time (76), potentially leading to poorer prognosis. Notably, MSLN shedding and other post-translational processing such as antigen maturation may result in discrepancies of MSLN expression at the RNA and protein levels, hence possibly explaining the different prognostic outcomes from the IHC and bulk RNA-seq data. Further validation using an independent Australian cohort is needed to determine whether the positive prognostic value of MSLN is reproducible and reflects a generalizable biological phenomenon or is influenced by population-specific genetic and/or environmental factors. The Australian population is racially and ethnically diverse and a comparison with other populations could be of interest.

Our finding that MSLN expression is associated with an immunosuppressive microenvironment is consistent with previous RNA-seq analyses (36, 50). In one study, a positive correlation between tumor MSLN expression and stromal CD274 (PD-L1) expression was found using the deconvoluted ICGC RNAseq data and validated in vitro (50). PD-L1, upon binding to the PD-1 receptor, is known to suppress T cell activating signals and inhibit anti-tumor responses (77). Although our study did not directly examine PD-1/PD-L1 signaling pathways, transcriptomic analyses of both mouse and human RNA-seq datasets revealed that MSLNhigh tumors exhibited decreased T cell activation signatures and suppressed tumor reactivity scores. However, in scRNA-seq, exhaustion phenotypes of CD8 T cells did not show significant differences between MSLN-high and MSLN-low groups. Downregulation of other immune-related pathways (such as leukocyte adhesion, proliferation and chemotaxis) was also observed in this study and suggests that additional immunosuppressive mechanisms could exist in MSLN-high tumors. In particular, we confirmed that expressions of chemokines and chemokine receptors that promote T cell migration and anti-tumor activities were suppressed in CD8 T cells from MSLN-high tumors, whereas expression of the immunosuppressive cytokine, CXCL5, was elevated. Furthermore, a reduced proportion of endothelial cells in the PLVAP+ venous

subtype was observed in the scRNA-seq dataset. PLVAP is known to regulate vascular permeability and facilitates leukocyte trafficking (78–80). Thus, decreased abundance of *PLVAP*+ endothelial cells could be linked to reductions in CD8 T cell infiltration as well.

In ovarian cancer, MSLN activates Wnt/β-catenin signaling to induce protumorigenic macrophage polarization via CD24 upregulation (81). While CD24 upregulation was not observed in our study from both the bulk RNA-seq and scRNA-seq analyses, we did find macrophages in MSLN-high tumors to exhibit increased polarization towards the tumorigenic M2 phenotype. MSLN overexpression has been shown to promote autocrine IL-6 signaling in PDAC cells (44); however, its association with cytokine signaling in T cells has not been specifically investigated. In our scRNA-seq analysis, we observed increased activity of proinflammatory cytokine signaling in CD8 T cells from MSLN-high tumors. Notably, this association was not identified in our bulk RNA-seq data, where such upregulated cytokine signaling activity may potentially be obscured by reduced infiltration of CD8 T cells. These suggest that high MSLN expression may be linked to broader immunomodulation within the PDAC TME, while the exact biological pathways underlying the observed functional changes in these immune infiltrates remain to be fully characterized.

High MSLN expression has been associated with reduced CD8 T cell infiltration in PDAC tumors in two independent human RNA-seq cohorts (TCGA and GSE62452) (36). Cell type compositions and immune activities were inferred based on the xCell algorithm (82). Although cohort-specific variations in multiple immune cell types, such as dendritic cells, were also observed, only CD8 T cells showed a consistent decrease in both RNA-seq cohorts. Suppressed immune responses (in lymphocyte infiltration, T-cell receptor richness, and cytolytic activity scores) were also associated with high MSLN expression. Nevertheless, cell type estimates and immune response predictions remain limited from bulk RNA-seq, as bona fide immune cell populations cannot be isolated for independent characterization. In the current study, estimates of cell type compositions from human RNA-seq samples demonstrated large discrepancies across the prediction tools used. Consequently, we confirmed CD8 T cell infiltration by scRNA-seq analysis as well as by IHC staining. Convincingly, as determined by scRNA-seq, CD8 T cells were the only immune subset that exhibited a significant reduction in abundance (~4% of total cells per sample, or 42% of total CD8 population) when comparing MSLN-high to MSLN-low tumors. The IHC validation also found a trend towards reduced CD8 T cell stromal infiltration but did not reach significance, likely due to the small sample size of this exploratory cohort (n = 10). Similarly, assessment of CD8 T cells using the MSLN cutoff defined in Section 3.1 (H-score = 62) showed an overall reduction in the MSLN-high group, but did not reach significance, likely due to the very limited number of cases remaining in this group after stratification (n = 3). The consistent inverse relationship between MSLN expression and CD8 T cell infiltration observed across multiple datasets warrants histopathological validation in larger independent cohorts in future studies.

It remains to be addressed whether there is a causative effect between MSLN expression and immunosuppression in PDAC. Our analysis on mouse RNA-seq data suggested that there was a lack of association between T cell infiltration status of the implanted tumor clones and tumor Msln levels. This suggests that immunosuppressive tumors did not cause upregulations of Msln expression. These findings, and whether high MSLN expression induces immunosuppression, remain to be tested in human-based experimental models. MSLN expression and CD8 T cell infiltration may also be specific to PDAC. Analyses in other MSLN-expressing tumors, such as mesothelioma, have interestingly indicated an opposite relationship where high MSLN expression was associated with high CD8 T cell density in TMAs (83). Transcriptomic analysis in ovarian and colorectal cancer also found higher CD8 T cell infiltration and higher T cell inflamed score, respectively, despite an overall positive association with an immunosuppressive tumor landscape (48, 49). Further studies to elucidate the mechanisms for MSLN and immuno-modulation are required, and to confirm whether this is a direct causative effect.

In summary, this study investigated the clinicopathological and prognostic significance of MSLN expression in an Australian PDAC cohort. A significant association between high MSLN expression and an immunosuppressive tumor microenvironment was also identified in PDAC, characterized specifically by reduced CD8 T cell infiltration. These findings have important clinical implications for treatment selection. Patients with low MSLN expression may derive greater benefit from immune checkpoint inhibitors (anti-PD-1 and anti-CTLA-4 antibodies) due to their relatively higher baseline CD8 T cell infiltration levels. Conversely, patients with high MSLN expression might be better candidates for MSLNtargeted therapies, such as the SS1P immunotoxin, given their increased target antigen expression. By elucidating the relationship between MSLN expression and immune contexture in PDAC, our work provides a foundation for developing more personalized treatment strategies that may improve patient outcomes.

### Data availability statement

The original contributions presented in the study are included in the article/Supplementary Material. Further inquiries can be directed to the corresponding author.

### **Ethics statement**

The studies involving humans were approved by University of Sydney Human Research Ethics Committee: 2018/730 and Sydney Local Health District Human Ethics Committee: 2020/ETH02321. The studies were conducted in accordance with the local legislation and institutional requirements. The ethics committee/institutional review board waived the requirement of written informed consent for participation from the participants or the participants' legal

guardians/next of kin because archived de-identified tissue and data was accessed.

### Author contributions

OL: Conceptualization, Data curation, Formal analysis, Validation, Visualization, Writing – original draft, Writing – review & editing, Methodology. ALW: Investigation, Methodology, Validation, Writing – review & editing. TF: Data curation, Investigation, Validation, Writing – review & editing. J-SS: Data curation, Investigation, Validation, Writing – review & editing. SMS: Supervision, Validation, Writing – review & editing. US: Methodology, Supervision, Visualization, Writing – review & editing. DY: Conceptualization, Funding acquisition, Methodology, Project administration, Supervision, Writing – review & editing.

### **Funding**

The author(s) declare financial support was received for the research and/or publication of this article. This work was funded by the RT Hall Trust (DY). OL is supported by the Postgraduate Research Scholarship in Building Expertise and Capability in Cell and Gene Therapies (New South Wales (NSW) Health and the University of Sydney). DY is supported by the Tour de Cure Mid-Career Grant (RSP-320); and Translational Partners Fellowship from Sydney Cancer Partners funded by Cancer Institute New South Wales (2021/CBG0002). US has received funding from the Australian National Health & Medical Research Council (1196405), the Tropical Australian Academic Health Centre (SF01124), and Townsville Hospital and Health Service (THHSSERTA\_RPG05\_2024 and THHSSERTA\_RPG15\_2024). The funders had no role in study design, decision to publish, or preparation of the manuscript.

### **Acknowledgments**

The authors thank the members of the Gene and Stem Cell Therapy Program, Centenary Institute and Department of Tissue Pathology and Diagnostic Oncology, Royal Prince Alfred Hospital, NSW Health Pathology for advice on experimental design and analysis. Biospecimens and clinical data were provided by the Australian Pancreatic Cancer Genome Initiative (APGI, www.pancreaticcancer. net.au) which is supported by an Avner Pancreatic Cancer Foundation Grant (www.avnersfoundation.org.au).

### Conflict of interest

The authors declare that the research was conducted in the absence of any commercial or financial relationships that could be construed as a potential conflict of interest.

The author(s) declared that they were an editorial board member of Frontiers, at the time of submission. This had no impact on the peer review process and the final decision.

### Generative AI statement

The author(s) declare that no Generative AI was used in the creation of this manuscript.

Any alternative text (alt text) provided alongside figures in this article has been generated by Frontiers with the support of artificial intelligence and reasonable efforts have been made to ensure accuracy, including review by the authors wherever possible. If you identify any issues, please contact us.

### Publisher's note

All claims expressed in this article are solely those of the authors and do not necessarily represent those of their affiliated organizations, or those of the publisher, the editors and the reviewers. Any product that may be evaluated in this article, or claim that may be made by its manufacturer, is not guaranteed or endorsed by the publisher.

### Supplementary material

The Supplementary Material for this article can be found online at: https://www.frontiersin.org/articles/10.3389/fimmu.2025.1651687/full#supplementary-material

### References

- 1. Sarantis P, Koustas E, Papadimitropoulou A, Papavassiliou AG, Karamouzis MV. Pancreatic ductal adenocarcinoma: Treatment hurdles, tumor microenvironment and immunotherapy. World J Gastrointest Oncol. (2020) 12:173–81. doi: 10.4251/wjgo.v12.i2.173
- 2. Bengtsson A, Andersson R, Ansari D. The actual 5-year survivors of pancreatic ductal adenocarcinoma based on real-world data. *Sci Rep.* (2020) 10:16425. doi: 10.1038/s41598-020-73525-y
- 3. Loveday BPT, Lipton L, Thomson BN. Pancreatic cancer: An update on diagnosis and management. *Aust J Gen Pract.* (2019) 48:826–31. doi: 10.31128/AJGP-06-19-4957
- 4. Hruban RH, Adsay NV, Albores-Saavedra J, Compton C, Garrett ES, Goodman SN, et al. Pancreatic intraepithelial neoplasia: a new nomenclature and classification
- system for pancreatic duct lesions. Am J Surg Pathol. (2001) 25:579–86. doi: 10.1097/00000478-200105000-00003
- 5. Muraki T, Jang KT, Reid MD, Pehlivanoglu B, Memis B, Basturk O, et al. Pancreatic ductal adenocarcinomas associated with intraductal papillary mucinous neoplasms (IPMNs) versus pseudo-IPMNs: relative frequency, clinicopathologic characteristics and differential diagnosis. *Mod Pathol.* (2022) 35:96–105. doi: 10.1038/s41379-021-00902-x
- 6. Elbanna KY, Jang HJ, Kim TK. Imaging diagnosis and staging of pancreatic ductal adenocarcinoma: a comprehensive review. *Insights Imaging*. (2020) 11:58. doi: 10.1186/s13244-020-00861-y

- 7. Ansari D, Gustafsson A, Andersson R. Update on the management of pancreatic cancer: surgery is not enough. World J Gastroenterol. (2015) 21:3157–65. doi: 10.3748/wig.v21.i11.3157
- 8. Janssen QP, O'Reilly EM, van Eijck CHJ, Groot Koerkamp B. Neoadjuvant treatment in patients with resectable and borderline resectable pancreatic cancer. *Front Oncol.* (2020) 10:41. doi: 10.3389/fonc.2020.00041
- 9. Jan IS, Ch'ang HJ. Selection of patients with pancreatic adenocarcinoma who may benefit from radiotherapy. *Radiat Oncol.* (2023) 18:137. doi: 10.1186/s13014-023-02328-v
- 10. Hassan R, Cohen SJ, Phillips M, Pastan I, Sharon E, Kelly RJ, et al. Phase I clinical trial of the chimeric anti-mesothelin monoclonal antibody MORAb-009 in patients with mesothelin-expressing cancers. *Clin Cancer Res.* (2010) 16:6132–8. doi: 10.1158/1078-0432.CCR-10-2275
- 11. Fujisaka Y, Kurata T, Tanaka K, Kudo T, Okamoto K, Tsurutani J, et al. Phase I study of amatuximab, a novel monoclonal antibody to mesothelin, in Japanese patients with advanced solid tumors. *Invest New Drugs*. (2015) 33:380–8. doi: 10.1007/s10637-014-0196-0
- 12. Lindenberg L, Thomas A, Adler S, Mena E, Kurdziel K, Maltzman J, et al. Safety and biodistribution of 111In-amatuximab in patients with mesothelin expressing cancers using single photon emission computed tomography-computed tomography (SPECT-CT) imaging. *Oncotarget*. (2015) 6:4496–504. doi: 10.18632/oncotarget.2883
- 13. Hassan R, Bullock S, Premkumar A, Kreitman RJ, Kindler H, Willingham MC, et al. Phase I study of SS1P, a recombinant anti-mesothelin immunotoxin given as a bolus I.V. infusion to patients with mesothelin-expressing mesothelioma, ovarian, and pancreatic cancers. *Clin Cancer Res.* (2007) 13:5144–9. doi: 10.1158/1078-0432.CCR-07-0869
- 14. Rottey S, Clarke J, Aung K, Machiels JP, Markman B, Heinhuis KM, et al. Phase I/IIa trial of BMS-986148, an anti-mesothelin antibody-drug conjugate, alone or in combination with nivolumab in patients with advanced solid tumors. *Clin Cancer Res.* (2022) 28:95–105. doi: 10.1158/1078-0432.CCR-21-1181
- 15. Beatty GL, O'Hara MH, Lacey SF, Torigian DA, Nazimuddin F, Chen F, et al. Activity of mesothelin-specific chimeric antigen receptor T cells against pancreatic carcinoma metastases in a phase 1 trial. *Gastroenterology*. (2018) 155:29–32. doi: 10.1053/j.gastro.2018.03.029
- 16. Yeo D, Giardina C, Saxena P, Rasko JEJ. The next wave of cellular immunotherapies in pancreatic cancer. *Mol Ther Oncolytics*. (2022) 24:561–76. doi: 10.1016/j.omto.2022.01.010
- 17. Haas AR, Tanyi JL, O'Hara MH, Gladney WL, Lacey SF, Torigian DA, et al. Phase I study of lentiviral-transduced chimeric antigen receptor-modified T cells recognizing mesothelin in advanced solid cancers. *Mol Ther.* (2019) 27:1919–29. doi: 10.1016/j.ymthe.2019.07.015
- 18. Golfier S, Kopitz C, Kahnert A, Heisler I, Schatz CA, Stelte-Ludwig B, et al. Anetumab ravtansine: a novel mesothelin-targeting antibody-drug conjugate cures tumors with heterogeneous target expression favored by bystander effect. *Mol Cancer Ther.* (2014) 13:1537–48. doi: 10.1158/1535-7163.MCT-13-0926
- 19. Carpenito C, Milone MC, Hassan R, Simonet JC, Lakhal M, Suhoski MM, et al. Control of large, established tumor xenografts with genetically retargeted human T cells containing CD28 and CD137 domains. *Proc Natl Acad Sci U S A.* (2009) 106:3360–5. doi: 10.1073/pnas.0813101106
- 20. Leshem Y, King EM, Mazor R, Reiter Y, Pastan I. SS1P immunotoxin induces markers of immunogenic cell death and enhances the effect of the CTLA-4 blockade in AE17M mouse mesothelioma tumors. *Toxins (Basel)*. (2018) 10:470. doi: 10.3390/toxins10110470
- 21. Klampatsa A, Dimou V, Albelda SM. Mesothelin-targeted CAR-T cell therapy for solid tumors. *Expert Opin Biol Ther*. (2021) 21:473–86. doi: 10.1080/14712598.2021.1843628
- 22. Chu Q. Targeting mesothelin in solid tumours: anti-mesothelin antibody and drug conjugates. Curr Oncol Rep. (2023) 25:309–23. doi: 10.1007/s11912-023-01367-8
- 23. Nagata K, Shinto E, Shiraishi T, Yamadera M, Kajiwara Y, Mochizuki S, et al. Mesothelin expression is correlated with chemoresistance in stage IV colorectal cancer. *Ann Surg Oncol.* (2021) 28:8579–86. doi: 10.1245/s10434-021-10507-y
- 24. Shiraishi T, Shinto E, Mochizuki S, Tsuda H, Kajiwara Y, Okamoto K, et al. Mesothelin expression has prognostic value in stage IotaIota/IotaIotaIota colorectal cancer. *Virchows Arch.* (2019) 474:297–307. doi: 10.1007/s00428-018-02514-4
- 25. Magalhaes I, Fernebro J, Abd Own S, Glaessgen D, Corvigno S, Remberger M, et al. Mesothelin expression in patients with high-grade serous ovarian cancer does not predict clinical outcome but correlates with CD11c(+) expression in tumor. *Adv Ther*. (2020) 37:5023–31. doi: 10.1007/s12325-020-01520-w
- 26. Cheng WF, Huang CY, Chang MC, Hu YH, Chiang YC, Chen YL, et al. High mesothelin correlates with chemoresistance and poor survival in epithelial ovarian carcinoma. *Br J Cancer*. (2009) 100:1144–53. doi: 10.1038/sj.bjc.6604964
- 27. Li YR, Xian RR, Ziober A, Conejo-Garcia J, Perales-Puchalt A, June CH, et al. Mesothelin expression is associated with poor outcomes in breast cancer. *Breast Cancer Res Treat.* (2014) 147:675–84. doi: 10.1007/s10549-014-3077-5
- 28. Parinyanitikul N, Blumenschein GR, Wu Y, Lei X, Chavez-Macgregor M, Smart M, et al. Mesothelin expression and survival outcomes in triple receptor negative breast cancer. Clin Breast Cancer. (2013) 13:378–84. doi: 10.1016/j.clbc.2013.05.001
- 29. Baba K, Ishigami S, Arigami T, Uenosono Y, Okumura H, Matsumoto M, et al. Mesothelin expression correlates with prolonged patient survival in gastric cancer. *J Surg Oncol.* (2012) 105:195–9. doi: 10.1002/jso.22024

- 30. Han SH, Joo M, Kim H, Chang S. Mesothelin expression in gastric adenocarcinoma and its relation to clinical outcomes. *J Pathol Transl Med.* (2017) 51:122–8. doi: 10.4132/jptm.2016.11.18
- 31. Thomas A, Chen Y, Steinberg SM, Luo J, Pack S, Raffeld M, et al. High mesothelin expression in advanced lung adenocarcinoma is associated with KRAS mutations and a poor prognosis. *Oncotarget*. (2015) 6:11694–703. doi: 10.18632/oncotarget.3429
- 32. Kachala SS, Bograd AJ, Villena-Vargas J, Suzuki K, Servais EL, Kadota K, et al. Mesothelin overexpression is a marker of tumor aggressiveness and is associated with reduced recurrence-free and overall survival in early-stage lung adenocarcinoma. *Clin Cancer Res.* (2014) 20:1020–8. doi: 10.1158/1078-0432.CCR-13-1862
- 33. Roe OD, Creaney J, Lundgren S, Larsson E, Sandeck H, Boffetta P, et al. Mesothelin-related predictive and prognostic factors in Malignant mesothelioma: a nested case-control study. *Lung Cancer*. (2008) 61:235–43. doi: 10.1016/j.lungcan.2007.12.025
- 34. Chu GJ, Linton A, Kao S, Klebe S, Adelstein S, Yeo D, et al. High mesothelin expression by immunohistochemistry predicts improved survival in pleural mesothelioma. *Histopathology.* (2023) 83:202–10. doi: 10.1111/his.14916
- 35. Montemagno C, Cassim S, Trichanh D, Savary C, Pouyssegur J, Pages G, et al. (99m)Tc-A1 as a novel imaging agent targeting mesothelin-expressing pancreatic ductal adenocarcinoma. *Cancers (Basel)*. (2019) 11:1531. doi: 10.3390/cancers11101531
- 36. Hagerty BL, Oshi M, Endo I, Takabe K. High Mesothelin expression in pancreatic adenocarcinoma is associated with aggressive tumor features but not prognosis. *Am J Cancer Res.* (2023) 13:4235–45.
- 37. Einama T, Kamachi H, Nishihara H, Homma S, Kanno H, Takahashi K, et al. Co-expression of mesothelin and CA125 correlates with unfavorable patient outcome in pancreatic ductal adenocarcinoma. *Pancreas*. (2011) 40:1276–82. doi: 10.1097/MPA.0b013e318221bed8
- 38. Winter JM, Tang LH, Klimstra DS, Brennan MF, Brody JR, Rocha FG, et al. A novel survival-based tissue microarray of pancreatic cancer validates MUC1 and mesothelin as biomarkers. *PloS One*. (2012) 7:e40157. doi: 10.1371/journal.pone.0040157
- 39. Le K, Wang J, Zhang T, Guo Y, Chang H, Wang S, et al. Overexpression of mesothelin in pancreatic ductal adenocarcinoma (PDAC). *Int J Med Sci.* (2020) 17:422–7. doi: 10.7150/ijms.39012
- 40. Chang K, Pastan I. Molecular cloning of mesothelin, a differentiation antigen present on mesothelium, mesotheliomas, and ovarian cancers. *Proc Natl Acad Sci U S A.* (1996) 93:136–40. doi: 10.1073/pnas.93.1.136
- 41. Bera TK, Pastan I. Mesothelin is not required for normal mouse development or reproduction.  $Mol\ Cell\ Biol.\ (2000)\ 20:2902-6.\ doi: 10.1128/MCB.20.8.2902-2906.2000$
- 42. Bharadwaj U, Li M, Chen C, Yao Q. Mesothelin-induced pancreatic cancer cell proliferation involves alteration of cyclin E via activation of signal transducer and activator of transcription protein 3. *Mol Cancer Res.* (2008) 6:1755–65. doi: 10.1158/1541-7786.MCR-08-0095
- 43. Bharadwaj U, Marin-Muller C, Li M, Chen C, Yao Q. Mesothelin confers pancreatic cancer cell resistance to TNF-alpha-induced apoptosis through Akt/PI3K/NF-kappaB activation and IL-6/Mcl-1 overexpression. *Mol Cancer*. (2011) 10:106. doi: 10.1186/1476-4598-10-106
- 44. Bharadwaj U, Marin-Muller C, Li M, Chen C, Yao Q. Mesothelin overexpression promotes autocrine IL-6/sIL-6R trans-signaling to stimulate pancreatic cancer cell proliferation. *Carcinogenesis*. (2011) 32:1013–24. doi: 10.1093/carcin/bgr075
- 45. Lurie E, Liu D, LaPlante EL, Thistlethwaite LR, Yao Q, Milosavljevic A. Histoepigenetic analysis of the mesothelin network within pancreatic ductal adenocarcinoma cells reveals regulation of retinoic acid receptor gamma and AKT by mesothelin. *Oncogenesis*. (2020) 9:62. doi: 10.1038/s41389-020-00245-3
- 46. Shimizu A, Hirono S, Tani M, Kawai M, Okada K, Miyazawa M, et al. Coexpression of MUC16 and mesothelin is related to the invasion process in pancreatic ductal adenocarcinoma. *Cancer Sci.* (2012) 103:739–46. doi: 10.1111/j.1349-7006.2012.02214.x
- 47. Chen SH, Hung WC, Wang P, Paul C, Konstantopoulos K. Mesothelin binding to CA125/MUC16 promotes pancreatic cancer cell motility and invasion via MMP-7 activation. *Sci Rep.* (2013) 3:1870. doi: 10.1038/srep01870
- 48. Li Y, Tian W, Zhang H, Zhang Z, Zhao Q, Chang L, et al. MSLN correlates with immune infiltration and chemoresistance as a prognostic biomarker in ovarian cancer. *Front Oncol.* (2022) 12:830570. doi: 10.3389/fonc.2022.830570
- 49. Malla M, Deshmukh SK, Wu S, Samec T, Olevian DC, El Naili R, et al. Mesothelin expression correlates with elevated inhibitory immune activity in patients with colorectal cancer. *Cancer Gene Ther*. (2024) 31:1547–58. doi: 10.1038/s41417-024-00816-1
- 50. LaPlante EL, Liu D, Petrosyan V, Yao Q, Milosavljevic A. XDec-CHI reveals immunosuppressive interactions in pancreatic ductal adenocarcinoma. *iScience*. (2022) 25:105249. doi: 10.1016/j.isci.2022.105249
- 51. Chan-Seng-Yue M, Kim JC, Wilson GW, Ng K, Figueroa EF, O'Kane GM, et al. Transcription phenotypes of pancreatic cancer are driven by genomic events during tumor evolution. *Nat Genet.* (2020) 52:231–40. doi: 10.1038/s41588-019-0566-9
- 52. Hendry S, Salgado R, Gevaert T, Russell PA, John T, Thapa B, et al. Assessing tumor-infiltrating lymphocytes in solid tumors: A practical review for pathologists and proposal for a standardized method from the international immunooncology

biomarkers working group: part 1: assessing the host immune response, TILs in invasive breast carcinoma and ductal carcinoma *in situ*, metastatic tumor deposits and areas for further research. *Adv Anat Pathol*. (2017) 24:235–51. doi: 10.1097/PAP.000000000000000

- 53. Quinlan AR, Hall IM. BEDTools: a flexible suite of utilities for comparing genomic features. *Bioinformatics*. (2010) 26:841-2. doi: 10.1093/bioinformatics/btq033
- 54. Dobin A, Davis CA, Schlesinger F, Drenkow J, Zaleski C, Jha S, et al. STAR: ultrafast universal RNA-seq aligner. *Bioinformatics*. (2013) 29:15–21. doi: 10.1093/bioinformatics/bts635
- 55. Liao Y, Smyth GK, Shi W. featureCounts: an efficient general purpose program for assigning sequence reads to genomic features. *Bioinformatics*. (2014) 30:923–30. doi: 10.1093/bioinformatics/btt656
- 56. Leek JT, Johnson WE, Parker HS, Jaffe AE, Storey JD. The sva package for removing batch effects and other unwanted variation in high-throughput experiments. *Bioinformatics*. (2012) 28:882–3. doi: 10.1093/bioinformatics/bts034
- 57. Li J, Byrne KT, Yan F, Yamazoe T, Chen Z, Baslan T, et al. Tumor cell-intrinsic factors underlie heterogeneity of immune cell infiltration and response to immunotherapy. *Immunity*. (2018) 49:178–93 e7. doi: 10.1016/j.immuni.2018.06.006
- 58. Peng J, Sun BF, Chen CY, Zhou JY, Chen YS, Chen H, et al. Single-cell RNA-seq highlights intra-tumoral heterogeneity and Malignant progression in pancreatic ductal adenocarcinoma. *Cell Res.* (2019) 29:725–38. doi: 10.1038/s41422-019-0195-y
- 59. Love MI, Huber W, Anders S. Moderated estimation of fold change and dispersion for RNA-seq data with DESeq2. *Genome Biol.* (2014) 15:550. doi: 10.1186/s13059-014-0550-8
- 60. Yu G, Wang LG, Han Y, He QY. clusterProfiler: an R package for comparing biological themes among gene clusters. *OMICS*. (2012) 16:284–7. doi: 10.1089/omi.2011.0118
- 61. Yan M, Hu J, Ping Y, Xu L, Liao G, Jiang Z, et al. Single-cell transcriptomic analysis reveals a tumor-reactive T cell signature associated with clinical outcome and immunotherapy response in melanoma. *Front Immunol.* (2021) 12:758288. doi: 10.3389/fimmu.2021.758288
- 62. Hanzelmann S, Castelo R, Guinney J. GSVA: gene set variation analysis for microarray and RNA-seq data. *BMC Bioinf.* (2013) 14:7. doi: 10.1186/1471-2105-14-7
- 63. Li T, Fu J, Zeng Z, Cohen D, Li J, Chen Q, et al. TIMER2.0 for analysis of tumor-infiltrating immune cells. *Nucleic Acids Res.* (2020) 48:W509–W14. doi: 10.1093/nar/gkaa407
- 64. Huang H, Wang Z, Zhang Y, Pradhan RN, Ganguly D, Chandra R, et al. Mesothelial cell-derived antigen-presenting cancer-associated fibroblasts induce expansion of regulatory T cells in pancreatic cancer. *Cancer Cell.* (2022) 40:656–73.e7. doi: 10.1016/j.ccell.2022.04.011
- 65. Zhang Z, Luo D, Zhong X, Choi JH, Ma Y, Wang S, et al. SCINA: A semi-supervised subtyping algorithm of single cells and bulk samples. *Genes (Basel)*. (2019) 10:531. doi: 10.3390/genes10070531
- 66. Cheng S, Li Z, Gao R, Xing B, Gao Y, Yang Y, et al. A pan-cancer single-cell transcriptional atlas of tumor infiltrating myeloid cells. *Cell.* (2021) 184:792–809.e23. doi: 10.1016/j.cell.2021.01.010
- 67. Andreatta M, Carmona SJ. UCell: Robust and scalable single-cell gene signature scoring. *Comput Struct Biotechnol J.* (2021) 19:3796–8. doi: 10.1016/j.csbj.2021.06.043
- 68. Andreatta M, Corria-Osorio J, Müller S, Cubas R, Coukos G, Carmona SJ. Interpretation of T cell states from single-cell transcriptomics data using reference atlases. *Nat Commun.* (2021) 12:2965. doi: 10.1038/s41467-021-23324-4

- 69. Jiang P, Zhang Y, Ru B, Yang Y, Vu T, Paul R, et al. Systematic investigation of cytokine signaling activity at the tissue and single-cell levels. *Nat Methods.* (2021) 18:1181–91. doi: 10.1038/s41592-021-01274-5
- 70. Hothorn T, Lausen B. On the exact distribution of maximally selected rank statistics. *Comput Stat Data Anal.* (2003) 43:121–37. doi: 10.1016/S0167-9473(02) 00225-6
- 71. Sun D, Tan L, Chen Y, Yuan Q, Jiang K, Liu Y, et al. CXCL5 impedes CD8(+) T cell immunity by upregulating PD-L1 expression in lung cancer via PXN/AKT signaling phosphorylation and neutrophil chemotaxis. *J Exp Clin Cancer Res.* (2024) 43:202. doi: 10.1186/s13046-024-03122-8
- 72. Inaguma S, Wang Z, Lasota J, Onda M, Czapiewski P, Langfort R, et al. Comprehensive immunohistochemical study of mesothelin (MSLN) using different monoclonal antibodies 5B2 and MN-1 in 1562 tumors with evaluation of its prognostic value in Malignant pleural mesothelioma. *Oncotarget*. (2017) 8:26744–54. doi: 10.18632/oncotarget.15814
- 73. Meyerhoff RR, Yang CF, Speicher PJ, Gulack BC, Hartwig MG, D'Amico TA, et al. Impact of mesothelioma histologic subtype on outcomes in the Surveillance, Epidemiology, and End Results database. *J Surg Res.* (2015) 196:23–32. doi: 10.1016/j.iss.2015.01.043
- 74. Liu X, Chan A, Tai CH, Andresson T, Pastan I. Multiple proteases are involved in mesothelin shedding by cancer cells. *Commun Biol.* (2020) 3:728. doi: 10.1038/s42003-020-01464-5
- 75. Johnston FM, Tan MC, Tan BRJr., Porembka MR, Brunt EM, Linehan DC, et al. Circulating mesothelin protein and cellular antimesothelin immunity in patients with pancreatic cancer. *Clin Cancer Res.* (2009) 15:6511–8. doi: 10.1158/1078-0432.CCR-09-0565
- 76. Staveley-O'Carroll K, Sotomayor E, Montgomery J, Borrello I, Hwang L, Fein S, et al. Induction of antigen-specific T cell anergy: An early event in the course of tumor progression. *Proc Natl Acad Sci U S A.* (1998) 95:1178–83. doi: 10.1073/pnas.95.3.1178
- 77. Sun C, Mezzadra R, Schumacher TN. Regulation and function of the PD-L1 checkpoint. *Immunity*. (2018) 48:434–52. doi: 10.1016/j.immuni.2018.03.014
- 78. Rantakari P, Auvinen K, Jappinen N, Kapraali M, Valtonen J, Karikoski M, et al. The endothelial protein PLVAP in lymphatics controls the entry of lymphocytes and antigens into lymph nodes. *Nat Immunol.* (2015) 16:386–96. doi: 10.1038/ni.3101
- 79. Keuschnigg J, Henttinen T, Auvinen K, Karikoski M, Salmi M, Jalkanen S. The prototype endothelial marker PAL-E is a leukocyte trafficking molecule. *Blood.* (2009) 114:478–84. doi: 10.1182/blood-2008-11-188763
- 80. Denzer L, Muranyi W, Schroten H, Schwerk C. The role of PLVAP in endothelial cells. *Cell Tissue Res.* (2023) 392:393–412. doi: 10.1007/s00441-023-03741-1
- 81. Zhong Y, Wang Y, Wang C, Cao K, Wang X, Xu X, et al. Targeting mesothelin-CD24 axis repolarizes tumor-associated macrophages to potentiate PD-1 blockade therapy in high-grade serous ovarian cancer. *J Immunother Cancer*. (2025) 13:e011230. doi: 10.1136/jitc-2024-011230
- 82. Aran D, Hu Z, Butte AJ. xCell: digitally portraying the tissue cellular heterogeneity landscape. *Genome Biol.* (2017) 18:220. doi: 10.1186/s13059-017-1349-1
- 83. Qualiotto AN, Baldavira CM, Balancin M, Ab'Saber A, Takagaki T, Capelozzi VL. Mesothelin expression remodeled the immune-matrix tumor microenvironment predicting the risk of death in patients with Malignant pleural mesothelioma. *Front Immunol.* (2023) 14:1268927. doi: 10.3389/fimmu.2023.1268927